Biochimica et Biophysica Acta 1837 (2014) 683–693

Contents lists available at ScienceDirect

Biochimica et Biophysica Acta

journal homepage: www.elsevier.com/locate/bbabio

Review

# Amino acid conservation and interactions in rhodopsin: Probing receptor activation by NMR spectroscopy ☆

Andreyah Pope [a], Markus Eilers [a], Philip J. Reeves [b], Steven O. Smith [a,*]

[a] Department of Biochemistry and Cell Biology, Stony Brook University, Stony Brook, NY 11794-5215, USA
[b] School of Biological Sciences, University of Essex, Wivenhoe Park, Essex CO4 3SQ, UK

ARTICLE INFO

*Article history:*
Received 16 July 2013
Received in revised form 15 October 2013
Accepted 18 October 2013
Available online 29 October 2013

*Keywords:*
Solid-state NMR spectroscopy
GPCR
Visual pigment

ABSTRACT

Rhodopsin is a classical two-state G protein-coupled receptor (GPCR). In the dark, its 11-*cis* retinal chromophore serves as an inverse agonist to lock the receptor in an inactive state. Retinal–protein and protein–protein interactions have evolved to reduce the basal activity of the receptor in order to achieve low dark noise in the visual system. In contrast, absorption of light triggers rapid isomerization of the retinal, which drives the conversion of the receptor to a fully active conformation. Several specific protein–protein interactions have evolved that maintain the lifetime of the active state in order to increase the sensitivity of this receptor for dim-light vision in vertebrates. In this article, we review the molecular interactions that stabilize rhodopsin in the dark-state and describe the use of solid-state NMR spectroscopy for probing the structural changes that occur upon light-activation. Amino acid conservation provides a guide for those interactions that are common in the class A GPCRs as well as those that are unique to the visual system. This article is part of a Special Issue entitled: Retinal Proteins — You can teach an old dog new tricks.



## 1. Introduction

### 1.1. Rhodopsin as a model class A GPCR

The class A receptors are the largest of five distinct classes of G protein-coupled receptors (GPCRs). These receptors have a common 7 transmembrane (TM) helix architecture and catalyze the exchange of GTP for GDP in intracellular heterotrimeric G proteins when activated. One of the intriguing questions surrounding GPCRs is how the 7-TM helix structure has evolved to be capable of responding to a diversity of signals. Rhodopsin, the low-light receptor in vertebrates, has often been considered an exception within the class A GPCRs, but is now providing the basis for a common mechanism for activation.

Rhodopsin serves as a model GPCR. The receptor functions as an on-off switch where light energy is used to drive the protein from an inactive to an active conformation. All visual receptors from humans to squid contain the 11-*cis* isomer of retinal covalently bound within the 7-TM helix bundle (Fig. 1). In pharmacological terms, the 11-*cis* retinal chromophore acts as a potent inverse agonist when bound to the receptor and reduces basal activity of the apo-protein opsin to very low levels [1,2]. Specific molecular interactions, including those involving 11-*cis* retinal, have evolved to lock this light-activated receptor into an inactive conformation in the dark, allowing the reduction of thermal "noise". Upon light absorption, the retinal isomerizes within 200 fs [3], and then decays thermally through a series of spectrally distinct intermediates. The Metarhodopsin II (Meta II) intermediate corresponds to the active state of the receptor. Like rhodopsin, Meta II is stabilized by specific contacts that enable sufficient time for G protein activation. Differences in these helix–helix interactions are what distinguish the highly sensitive rhodopsin receptors that function in dim-light from the cone pigments that operate in ambient light conditions and require faster response and recovery times [4].

In the transition from Meta I to Meta II, the receptor undergoes a large conformational change. EPR studies revealed that there is an outward rotation of the cytoplasmic end of TM helix H6 in the transition to Meta II [5]. The motion of H6 opens up a cavity on the intracellular side of the receptor that serves as the G-protein binding pocket. The crystal structures of active opsin [6,7] showed that the outward rotation of H6 is accompanied by rotation of the intracellular portions of TM helices H5 and H7. Specific contacts between conserved tyrosines on these helices with Arg135 on helix H3 serve to stabilize H6 in an open conformation. The mechanism for how retinal isomerization is coupled to motion of helices H5, H6 and H7, however, is only now being unraveled.

### 1.2. NMR provides a complementary approach to X-ray crystallography

Rhodopsin was the first GPCR whose crystal structure was determined at high resolution [8]. The structure confirmed the seven-helix

☆ This article is part of a Special Issue entitled: Retinal Proteins — You can teach an old dog new tricks.

* Corresponding author. Fax: +1 631 632 8575.
*E-mail address:* steven.o.smith@stonybrook.edu (S.O. Smith).

0005-2728/$ – see front matter © 2013 Elsevier B.V. All rights reserved.
http://dx.doi.org/10.1016/j.bbabio.2013.10.007

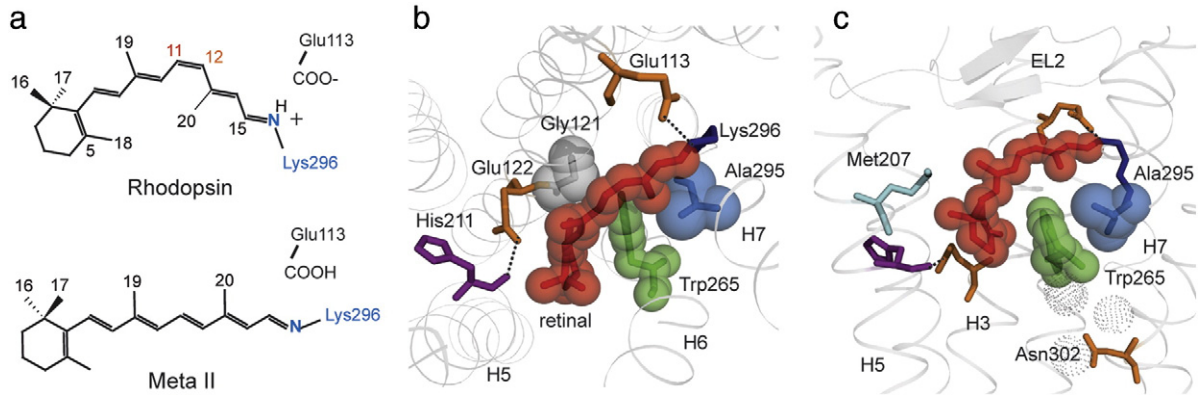


**Fig. 1.** Packing interactions of the retinal chromophore in rhodopsin. (a) Structures of the 11-*cis* retinal chromophore in rhodopsin and the all-*trans* retinal chromophore in the active intermediate, Meta II. (b, c) Two views of the structure of the retinal-binding pocket in rhodopsin (PDB ID: 1GZM). The view from the extracellular surface (b) shows several of the molecular interactions that lock the receptor in the inactive conformation in the dark. These include the Glu113–retinal PSB electrostatic interaction, the Glu122 – His211 hydrogen bonding interaction and the close van der Waals packing interaction between Trp265 and the retinal polyene chain. The view of the binding site from the membrane clearly shows how Trp265 is tightly packed between the retinal, Ala295 and Gly121. Ala295 is group-conserved across the class A GPCRs, while Gly121 is highly conserved within the opsin subfamily of receptors. The indole side chain of Trp265 is hydrogen bonded to Asn302 via water molecules (dotted spheres).

architecture and revealed the location of amino acids that are highly conserved across the large class A GPCR family. In the past 8 years a number of high-resolution crystal structures of class A GPCRs have been determined, mainly in their inactive forms. In addition to the visual pigments [6,7,9,10], high-resolution structures have been determined for amine [11–21], chemokine [22], mAChR [23,24], opioid [25–28], lipid [29] and δ-subfamilies of receptors [30], the latter including the olfactory receptors. The basic structural elements present in these structures are similar to those observed in rhodopsin. Comparison of rhodopsin with the ligand activated GPCRs shows that the largest structural diversity occurs in the N-terminus, the extracellular loops and the intracellular loops. On the extracellular side of rhodopsin, the second extracellular loop (EL2) is wedged between the TM helices and serves as a cap on the retinal-binding site. On the intracellular side, a short amphipathic helix is oriented roughly perpendicular to the seven TM helices.

In contrast, crystal structures of active GPCRs are fewer in number. Active state crystal structures of ligand-activated receptors that exhibit a large outward motion of H6 have been determined for the β2-adrenergic receptor with either a nanobody or the full length G protein bound to the intracellular surface [31,32]. In the presence of agonist alone, the structural changes in the ligand-activated GPCRs are more modest [15,33]. These receptors have relatively small barriers to activation in contrast to rhodopsin where light energy is needed to overcome the large thermal barrier to activation. In most GPCRs, multiple receptor conformations can be populated, which provides versatility in signaling and regulation [34].

Agonist-bound structures are available for the $A_{2A}$ adenosine receptor [15,35], the $\beta_1$ adrenergic receptor ($\beta_1$AR) [33,36], the $\beta_2$ adrenergic receptor ($\beta_2$AR) [37] and the $\beta_2$AR in complex with Gs [32,38]. The largest change in these structures, as compared to the corresponding inactive conformation, is the displacement of TM helix H6. Agonist-induced conformational changes in other regions of these receptors appear to be minimal, which has left open the question as to how ligand binding triggers activation [39,40].

In order to correlate structure with function in GPCRs, a detailed understanding of the subtle differences between the various receptor conformations is required. High-resolution structural data are needed for each receptor state in as close to a native conformation as possible. Solid-state NMR spectroscopy has been particularly useful in characterizing the structure of dark rhodopsin and its intermediates. Deuterium NMR spectroscopy along with molecular dynamics has provided insights into the structure and dynamics of the retinal chromophore [41], while $^{13}C$ and $^{1}H$ NMR correlation spectroscopy has been used to probe the retinal structure and its interaction with surrounding amino acids [42,43] The use of selective pairs of $^{13}C$ labels has been useful for characterizing the conformation of the retinal [44] and internuclear $^{13}C\ldots^{13}C$ distances in the protein [45]. The receptor structure can be probed in a membrane environment using the native protein sequence or site directed mutants, and low temperature [46] provides a way to trap intermediates. In this review, we describe the use of solid-state NMR in the context of understanding the molecular interactions that stabilize the active and inactive states of rhodopsin. We highlight the retinal chromophore and its interactions with His211 on H5 and Trp265 on H6 to illustrate the types of structural information that can be obtained by NMR.

### *1.3. Molecular interactions and residue conservation provide insights into mechanism*

Understanding the roles of the residues that are conserved across the class A GPCR family is an important component for developing a comprehensive description of the activation mechanism of rhodopsin. There are three levels of conservation that one must consider. The first level of conservation corresponds to the ~20 signature residues that have high sequence identity across the class A GPCRs. These residues are often grouped into structural and functional micro-domains that appear to mediate a common conformational switch involved in receptor activation. A second level of conservation corresponds to those residues that are highly conserved when considered as a group of similar amino acids. We have previously identified the group of small and weakly polar residues (Ala, Gly, Ser, Cys and Thr) as key determinants in helix–helix interactions [47,48]. However, there are other classifications of group-conserved amino acids, such as aromatic, charged or hydrophobic. The third level of conservation corresponds to those residues that are highly conserved within a receptor subfamily.

For example, in rhodopsin an aromatic cluster of amino acids is found on H6, which has relatively high sequence identity across the class A GPCRs. Trp265 lies within the arc formed by the retinal polyene chain and the Lys296 side-chain, and is packed between Gly121 and Ala295 (Fig. 1). Gly121 and Lys296 are highly conserved in the visual receptor subfamily and Ala295 is a group-conserved residue across the class A GPCRs. The 11-*cis* retinal appears to function as a clamp to prevent motion of Trp265 and H6 [49], thus locking the dark-state conformation. Isomerization of the retinal and motion of the β-ionone ring toward H5 appear to be essential for motion of Trp265 [49]. Together, the conserved amino acids form a network spanning all seven

transmembrane helices and mediate the conformational switch(es) that governs activation of the class A GPCRs.

## 2. Packing interactions involving the retinal chromophore

### 2.1. Retinal isomerization triggers receptor activation

The 11-*cis* retinal ligand is attached to Lys296 through a protonated Schiff base (PSB) linkage. The positive charge created by protonation of the Schiff base increases electron delocalization along the conjugated retinylidene chain and shifts the absorption band from the short wavelength range into the middle of the visible spectrum. The protein counterion to the positive charge is Glu113 on helix H3. The Glu113–PSB salt bridge is crucial not only for wavelength regulation, but also for maintaining the receptor in an inactive conformation. Proton transfer from the PSB to Glu113 is an essential element in triggering receptor activation [50] and is explained further in Section 5.

The 11-*cis* retinal chromophore is longitudinally restricted within its binding pocket. The shape of this binding pocket imparts a twist about the C11 – C12 double bond of the 11-*cis* retinal that guides the *cis* to *trans* isomerization within this constrained binding site. Deuterium measurements on the retinal reveal that the C20 methyl group is displaced out of the retinal plane and provided evidence for the 'pretwist' about the C11 – C12 double bond [51,52]. This conformational distortion "primes" the retinal for isomerization [53–55].

NMR measurements of dipolar interactions between $^{13}$C sites along the retinal provide support for conformational distortions in its ground state structure. Such measurements yield a value of 160° ± 10° for the H – C10 – C11 – H torsion angle in rhodopsin [56] and 180° ± 25° in the Meta I intermediate [57] indicating that this region of the retinal has relaxed following isomerization. A twist about the C10 – C11 bond in the ground state is consistent with data from rotational resonance experiments measuring the distance between the C20 methyl group and the polyene chain in rhodopsin and in the Meta I intermediate [58]. Double quantum filtering (DQF) methods greatly enhance the signal arising from enriched directly bonded $^{13}$C pairs relative to the natural abundance $^{13}$C signals and have provided an avenue for studies of retinal conformation.

Both the retinal polyene chain and its associated methyl groups contribute to the ability of the retinal to trigger activation. Steric interactions involving the retinal C19 and C20 methyl groups influence activation. The C20 methyl group in rhodopsin contacts Trp265 and Tyr268 on H6 in the dark state. When the retinal C20 methyl group is removed, the photoreaction is slowed [59] and the quantum yield is reduced [60]. The retinal C19 methyl group in rhodopsin is tightly constrained in the retinal binding site and packs against Thr118, Ile189, Tyr191 and Tyr268. Removal of the C19 methyl group prevents receptor activation [61], while replacement of the retinal C19 methyl group with an ethyl or propyl group converts the 11-*cis* PSB chromophore from a potent inverse agonist into a partial agonist, with the amount of activity being proportional to the size of the substituent at the C19 position [62].

Fig. 2 presents two-dimensional solid-state NMR spectra illustrating the contacts between the retinal C19 and C20 methyl groups and Trp265 in rhodopsin and Meta II. The experiments were run with the retinal $^{13}$C-labeled at the C19 or C20 methyl groups and $^{13}$C-labels on tryptophan residues in the protein. The $^{13}$C-labeled tryptophan was introduced by expressing rhodopsin using defined media containing selectively labeled amino acids [63]. The $^{13}$C-labeled retinal was

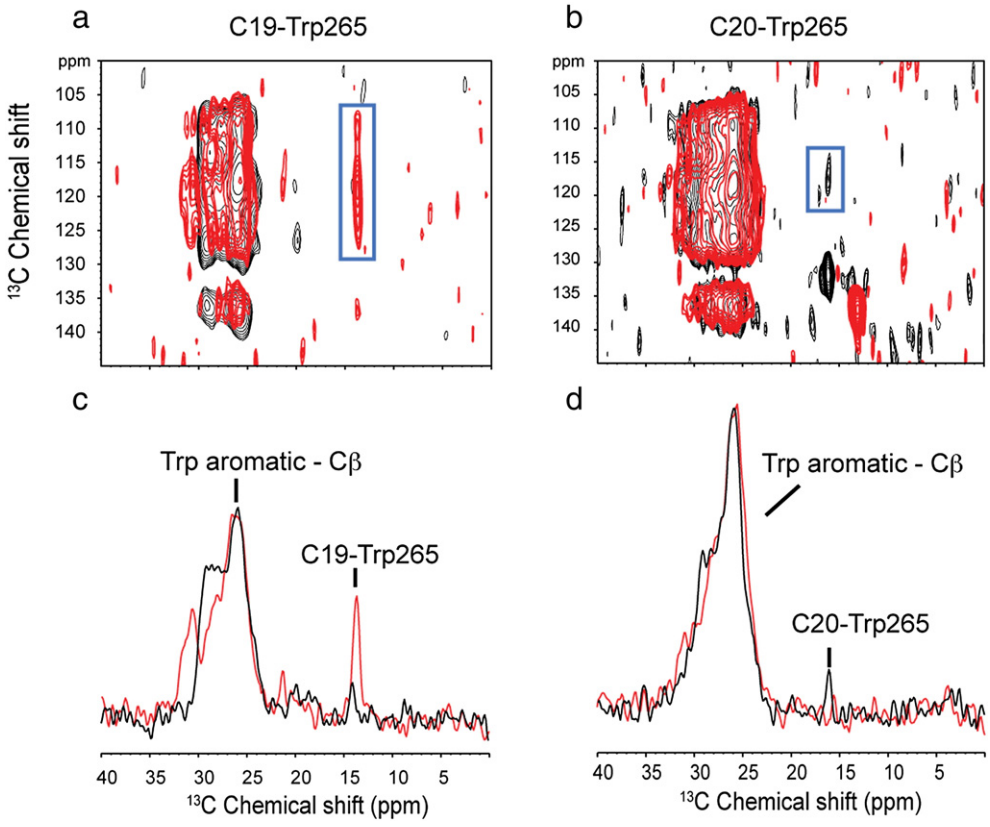


**Fig. 2.** Solid-state NMR spectroscopy of rhodopsin and Meta II illustrating changes in retinal–Trp265 contacts. (a, b) Regions of the two-dimensional DARR NMR spectra used to obtain internuclear contacts. This region of the spectrum corresponds to cross peaks within the Trp side chain and between Trp265 and the retinal C19 and C20 methyl groups. In addition, for the experiment in panel (b), the retinal was $^{13}$C labeled at both C12 and C20. The close $^{13}$C12…$^{13}$C20 distance (~2.5 Å) results in large cross peaks for rhodopsin (black, ~132 ppm) and Meta II (red, ~138 ppm). The contour plot in (b) was scaled to observe the weak C20 – Trp265 cross peak, resulting in an increase in noise. (c, d) One-dimensional rows extracted from the 2D spectra shown in panels (a) and (b). The rows clearly show the intensity differences, which are used to estimate internuclear distance.

introduced by regenerating the opsin apo-protein with synthetic retinal containing specific $^{13}$C-labels. This labeling strategy introduces sparse $^{13}$C sites throughout the protein, allowing us to measure $^{13}$C…$^{13}$C distances via the measurement of $^{13}$C…$^{13}$C dipolar couplings. Structural constraints in NMR spectroscopy are often in the form of internuclear distance. Magic angle spinning (MAS), which is used to obtain high resolution NMR spectra of membrane proteins by solid-state NMR, averages dipolar couplings with magnitudes on the order of or less than the MAS frequency. Selective reintroduction of dipolar couplings, while retaining the high resolution of MAS, allows internuclear distance measurements using the $1/r^3$ distance dependence of the dipolar interaction. Several methods have been developed to reintroduce dipolar couplings under MAS conditions in order to measure distances [64–70]. However, we have found dipolar assisted rotational resonance (DARR) NMR, which is based on spin diffusion, to be the most effective method to obtain distances in $^{13}$C-labeled membrane proteins [71]. DARR allows polarization transfer in a manner that is relatively insensitive to the chemical shift differences [70]. Typically, the 2D $^{13}$C DARR spectrum is shown as a contour plot with diagonal resonances and off diagonal cross peaks. The off-diagonal cross peaks arise from $^{13}$C sites that separated in space by less than ~6–7 Å. The intensity of the cross peaks is inversely related to internuclear distance. For simplicity, we often only show rows through the cross peaks, which allows one to estimate their relative intensities.

In Fig. 2, we present both 2D contour plots and rows through the 2D spectra in the region of the retinal–Trp cross peaks. The spectra of rhodopsin (black) and Meta II (red) are superimposed. The large resonances in the 2D spectra correspond to intra-residue cross peaks between the Cβ carbons of the 5 tryptophan residues and the aromatic carbons of the indole ring. The smaller resonances (blue box) correspond to the specific cross peaks between the retinal C19 or C20 methyl carbons and Trp265. There are two features of these spectra that emerge from a comparison of the C19 and C20 cross peak intensities. First, the C20–Trp intensity is weak, indicating a relatively long intermolecular distance. In an independent study, de Groot and colleagues observed a correlation between C8 and Trp265 in rhodopsin, but were not able to observe the edge-on contact with the C20 methyl group even though the distances (~3.9 Å) are comparable [42]. Second, in the contour plots it is clear that the C20 methyl group is coupled to only a single carbon of the aromatic ring. In contrast, the C19 methyl group is coupled to several aromatic carbons. This comparison indicates that the C20 methyl group is oriented toward the edge or end of the indole ring (consistent with the crystal structure of dark rhodopsin), whereas the C19 methyl group is in van der Waals contact (or very closely packed) to the surface of the indole ring (i.e., the intensity of the inter-residue C19–Trp cross peak approaches that of the intra-residue Trp cross peaks).

### 2.2. Orientation of the retinal chromophore in Meta II

In the past few years, several crystal structures have been reported on the active Meta II state of rhodopsin [9,72,73]. Two structures have been reported on rhodopsin containing mutations (E113Q and M257Y) that lead to constitutive activation [50,51]. These structures were obtained with the all-*trans* retinal chromophore present in the retinal-binding site. In the E113Q structure, the all-*trans* retinal was not covalently attached. In the M257Y structure, the all-*trans* retinal was attached as an unprotonated Schiff base to Lys296. In the third Meta II structure, all-*trans* retinal was added to crystals of opsin to generate a Meta II-like complex. In this opsin–retinal complex and the M257Y structure, the orientation of the retinal is different than the orientation proposed on the basis of solid-state NMR measurements.

An analysis of the cross-peak intensities in Fig. 2 provides a point of comparison between the crystal structures and Meta II studied by NMR. The intensity of the retinal–C20 cross peak is consistent with the crystal structure of rhodopsin showing that the C20 methyl group is oriented edge-on to the Trp side chain. The closest carbon (Cζ3) is 3.9 Å away. The relatively weak intensity is due to dipolar truncation (which occurs when measuring a weak through-space interaction in the presence of a strongly coupled system, in this case the uniformly $^{13}$C-labeled tryptophan) [74]. Comparison with crystal structures of Meta II shows that the C19 methyl group is still oriented approximately edge-on to the Trp265 indole side chain. The C19–Trp distance is longer in the structure of "wild-type" Meta II (3PQR) than in rhodopsin [9], which is inconsistent with the measured intensities. The distance is closer in the structure of the M257Y mutant of Meta II [73]. However, the orientation still results in only 1 or 2 carbons being relatively close to the Trp265 indole ring.

Meta II involves at least two substates, referred to as Meta IIa and Meta IIbH+ [75]. The first corresponds to the outward rotation of H6 and the second protonation of Glu134 in the conserved ERY sequence on H3. Once Arg135 is stabilized by the inward rotation of Tyr223 and Tyr306, the retinal is hydrolyzed and can leave the binding pocket. In the solid-state NMR experiments, we trap Meta II following protonation of Glu134 (substate Meta IIbH+), but prior to Schiff base hydrolysis. The retinal chemical shifts at the opposite ends of the polyene chain (C5 and C15) are unusual [76]. For example, the retinal C5 chemical shift is upfield compared to that in model retinal Schiff bases. The upfield chemical shift suggests that the C5C6C7C8 torsion angle (which connects the β-ionone ring to the retinal polyene chain) is appreciably non-planar Meta II. The non-planar angle would be consistent with steric interactions between the ring and residues on TM helix H5. In addition, $^{1}$H and $^{13}$C MAS NMR have provided evidence for strong steric interactions between β-ionone ring of the retinal chromophore and surrounding aromatic residues [43]. We have suggested that relaxation of the retinal and surrounding protein occurs upon retinal hydrolysis [76]. This relaxed state associated with opsin may be more amenable to X-ray crystallography.

### 2.3. Packing and position of Trp265 in rhodopsin and Meta II

The orientation of the retinal has implications on the position of the Trp265 side chain in Meta II. In the static crystal structures of Meta II [9,72,73] and of activated GPCRs [15,32,36–38], the conserved Trp residue has not shifted significantly from its position in the inactive state. These data suggest that the tryptophan serves as an anchor point on the helix. In contrast, there are several studies, using experimental systems that do not require crystallization, which have argued for larger changes in the position of the tryptophan upon activation.

Chabre and Breton [77] used linear dichroism to show that at least one of the five tryptophans changes orientation upon retinal isomerization. Rafferty and coworkers [78] interpreted UV–Vis difference bands that appear in the formation of Meta II as resulting from two tryptophans moving into more polar environments. Lin and Sakmar were able to assign the peaks observed in the UV–Vis difference spectra to specific tryptophans by combining optical spectroscopy with site-directed mutagenesis [79]. They found that the difference bands at 294 nm and 302 nm are associated with changes in the environments of Trp126 and Trp265. Importantly, Trp35 and Trp175 do not contribute to the difference spectra, while Trp161 contributes only slightly. Based on comparison to model compounds, they attributed the absorption changes to decreased hydrophobicity or polarizability in Meta II, and weaker hydrogen bonding interactions of the indole NH groups. These conclusions parallel those using UV Raman spectroscopy [80].

Fig. 3a shows the hydrogen bonding interactions of Trp265 with structural waters (dotted van der Waals spheres) surrounding Asn302. Solid-state NMR of $^{15}$N–Trp-labeled rhodopsin provides a more direct assessment of the hydrogen bonding of the indole N–H groups [81]. Fig. 3b presents the $^{15}$N MAS spectrum for wild-type rhodopsin (black) containing tryptophan uniformly labeled with $^{13}$C and $^{15}$N. Both the backbone amide and sidechain indole of the five Trp residues are $^{15}$N-labeled. The $^{15}$N spectrum of rhodopsin shows five distinct

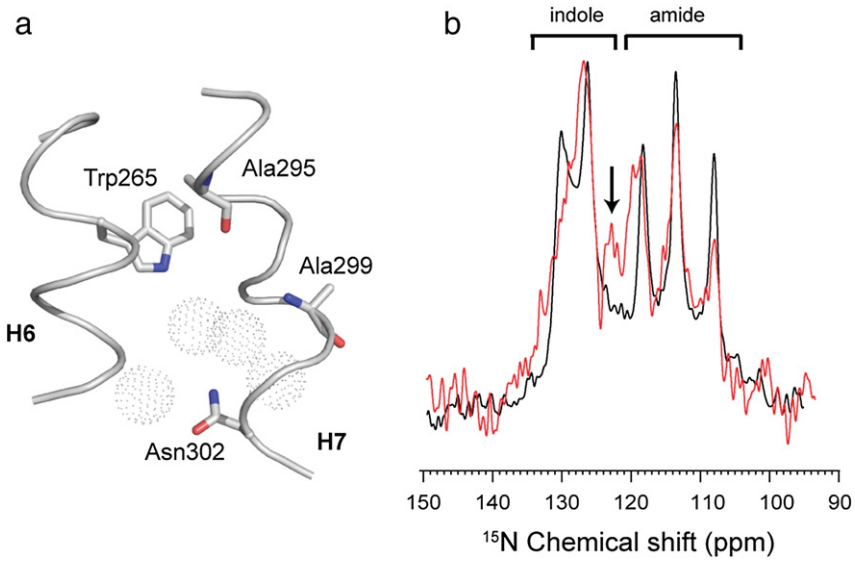


**Fig. 3.** Hydrogen bonding changes of tryptophan indole NH groups. (a) Structural waters located between the indole NH of Trp265 and the side chain amide of Asn302 mediate hydrogen-bonding interactions between these two highly conserved residues. (b) $^{15}$N NMR spectra are shown corresponding to the indole NH resonances of tryptophan in rhodopsin (black) and Meta II (red). The Trp126 resonance at 130 ppm shifts to 128 ppm, while the Trp265 resonance shifts from 127 ppm to 123 ppm (marked with arrow).

resonances on top of a broad component. On the basis of their chemical shifts, the three resolved resonances between 105 and 120 ppm are assigned to backbone amide nitrogens and the two resolved resonances between 125 and 133 ppm are assigned to indole nitrogens [82]. Integration of the intensity of each peak shows an approximate 2:1:1:1:1 ratio after subtracting the broad component. This intensity ratio suggests that only three of the five tryptophans are resolved and that the other two tryptophans contribute to the unresolved broad baseline [81]. Mutational studies on the Trp residues allow us to assign Trp126 as the most downfield shifted Trp consistent with strong hydrogen bonding with Glu122 in rhodopsin ([81], unpublished data). Trp265 is the most upfield shifted Trp consistent with hydrogen bonding to structural water.

Fig. 3b also presents the $^{15}$N MAS spectrum of wild-type Meta II (gray). Comparison of wild-type dark rhodopsin with Meta II reveals changes mainly in the chemical shifts of the indole nitrogens. The $^{15}$N resonances of the amide nitrogens are broadened slightly in Meta II, but are at the same frequencies as in rhodopsin. In contrast, in the indole region of the spectrum there is a loss of intensity at ~130 ppm and a gain of intensity at 123 ppm and 127 ppm. Griffin and coworkers [83] have shown that the chemical shift of the indole nitrogen in tryptophan model compounds and bacteriorhodopsin is correlated with hydrogen bond strength. Decreased hydrogen-bonding results in a shift of the indole $^{15}$N resonance to lower $^{15}$N frequency. Based on the observed shift of two of the indole $^{15}$N resonances to lower $^{15}$N frequency in Fig. 3, we conclude that at least two tryptophans in the TM region become more weakly hydrogen bonded in Meta II. We have assigned these to Trp126 and Trp265. Trp126 becomes more weakly hydrogen bonded as the Glu122 side chain switches hydrogen-bonding interactions to the side chain of His211 in Meta II. The hydrogen bonding changes of Trp265 are more difficult to explain on the basis of the crystal structures of Meta II, where the Trp265 side chain remains oriented in roughly the same position as in rhodopsin.

## 3. Amino acid conservation and packing within the TM core of rhodopsin

Most of the highly conserved residues in the class A GPCR family are located in the TM helices (Table 1). The "signature" amino acids with sequence identities of >70% are the most important set of conserved residues in the class A GPCR family. The conserved prolines on H5, H6 and H7, along with the (E/D)RY and NPxxY motifs, have been extensively studied. Several hydrophobic residues (e.g., Trp161 and Leu79) are highly conserved, but less well studied because it has not been clear how they are involved in receptor structure or function. To understand the role of the signature residues, it is important to consider helix packing and the positions of water, as well as their position relative to the group-conserved residues described above.

Fig. 4 highlights the packing interactions of the seven TM helices in rhodopsin and opsin. The helices are color-coded based on their overall packing value determined by taking the average packing value of the individual amino acids in each helix. H3 has the highest packing value, while H5 has the lowest overall packing value. We have previously suggested that helices H1–H4 (and possibly H7) form a tightly packed core on the basis of the location of the group-conserved positions [47,48].

**Table 1**
Amino acid conservation in class A GPCRs.

| Signature conserved | | Packing values | Group conserved | | Packing values |
|---|---|---|---|---|---|
| Asn55$^{1.50}$ | 99.5% | 0.624 | Gly51$^{1.46}$ | 92.5% | 0.619 |
| Leu79$^{2.50}$ | 94.0% | 0.486 | Ile54$^{1.49}$ | 77.7% | 0.464 |
| Ala80$^{2.51}$ | 97.4% | 0.574 | Ala82$^{2.53}$ | 82.2% | 0.552 |
| Asp83$^{2.54}$ | 89.4% | 0.582 | Ala124$^{3.39}$ | 77.9% | 0.472 |
| Cys110$^{3.25}$ | 89.2% | 0.654 | Ala132$^{3.47}$ | 99.7% | 0.528 |
| Leu128$^{3.43}$ | 77.6% | 0.497 | Ala153$^{4.42}$ | 81.0% | 0.529 |
| Glu134$^{3.49}$ | 71.7% | 0.522 | Ala164$^{4.53}$ | 92.6% | 0.610 |
| Arg135$^{3.50}$ | 98.1% | 0.514 | Ala168$^{4.57}$ | 87.5% | 0.668 |
| Tyr136$^{3.51}$ | 71.6% | 0.467 | Ala295$^{7.42}$ | 83.4% | 0.596 |
| Trp161$^{4.50}$ | 88.4% | 0.411 | Ala299$^{7.42}$ | 78.0% | 0.529 |
| Cys187$^{EL2}$ | 87.4% | 0.676 | | | |
| Pro215$^{5.42}$ | 72.8% | 0.636 | | | |
| Tyr223$^{5.50}$ | 93.2% | 0.250 | | | |
| Pro267$^{6.50}$ | 80.1% | 0.351 | | | |
| Asn302$^{7.49}$ | 85.7% | 0.422 | | | |
| Pro303$^{7.50}$ | 98.1% | 0.500 | | | |
| Tyr306$^{7.53}$ | 93.2% | 0.585 | | | |
| Trp265$^{6.48}$ | 69.2% | 0.575 | | | |

a. Conservation was calculated on the basis of the most recent alignments in the GPCR database. b. The packing values were calculated using the method of occluded surfaces. c. The superscripts correspond to the generic numbering system developed by Ballesteros and Weinstein (e.g., Trp265$^{6.48}$) that gives the position of an amino acid relative to the most conserved amino acid on a specific helix. In this example, the superscript 6.48 indicates that Trp265 is two residues toward the N terminus of the most conserved residue (designated 50) on H6 (i.e., Pro267$^{6.50}$).

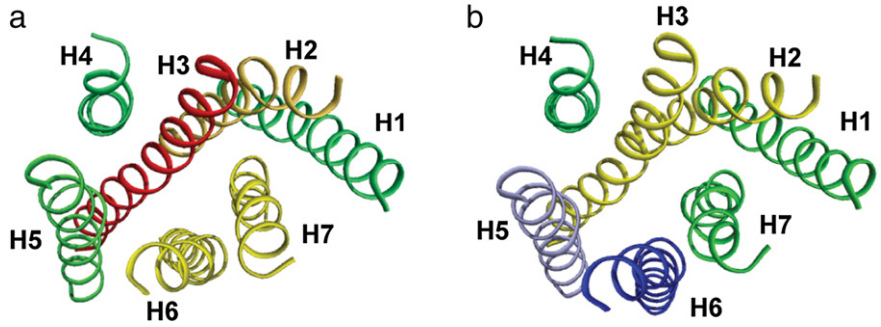


**Fig. 4.** Helix packing in rhodopsin and active opsin. The seven TM helices are color coded according to the average packing values of the residues in each helix for rhodopsin (PDB ID: 1U19) and active opsin (PDB ID: 3CAP). The packing values were calculated using the method of occluded surfaces [90]. For reference, the average packing value for residues in TM helices is ~0.44 [48]. Red (>0.495), orange (0.494–0.475), orange-yellow (0.474–0.455), yellow (0.454–0.435), lime green (0.434–0.415), green (0.414–0.395), light blue (0.394–0.375), and blue (<0.375).

Fig. 5a presents a cross section through the middle of the TM region of rhodopsin illustrating the conserved packing core. The core is composed of both signature (red) and group conserved (blue) amino acids. The most highly conserved residue in the class A GPCRs is Asn55. Close analysis of the amide functional group shows that the amine $NH_2$ is hydrogen bonded to the backbone carbonyls of Gly51 on TM helix H1 and Ala299 on H7, both group conserved amino acids. Asp83 is part of the highly conserved LAxAD sequence on TM helix H2. Leu79 and Asp83 are signature residues, while Ala80 and Ala82 are group conserved. The very high group conservation of Ala80 (97%) allows close H1–H2 packing and the formation of a specific Asn55–Asp83 hydrogen bonding contact. Ala82 mediates the packing of helix H2 with helices H3 (Ile123) and H4 (Trp161). Together, Ala82 and Ile123 form a pocket that allows hydrogen bonding of Trp161 (indole NH) to Asn78, thereby bridging H2 and H4. Fig. 5b shows the conformational changes in the packing core upon activation. An analysis of the hydrogen bonding interactions of Trp161 indicates that it does not change upon activation, although the crystal structures of opsin and Meta II show a change in conformation. The most dramatic change is a closing of the space between Leu128 and Asn302 as H6 pivots outward, displacing Met257.

For comparison, the packing core in the inactive and active conformations of the $\beta_2$AR is shown in Fig. 5c and d. These figures illustrate how a crevice created by Ala78 on H2 and Ala119 on H3, both group conserved residues, allows the docking of Trp158. In this case, the indole NH of Trp158 is hydrogen bonded to the side chain of Ser74. This comparison shows that a key polar residue precedes the LAxAD motif on H2 in both rhodopsin and the $\beta_2$AR. As with rhodopsin, the most dramatic

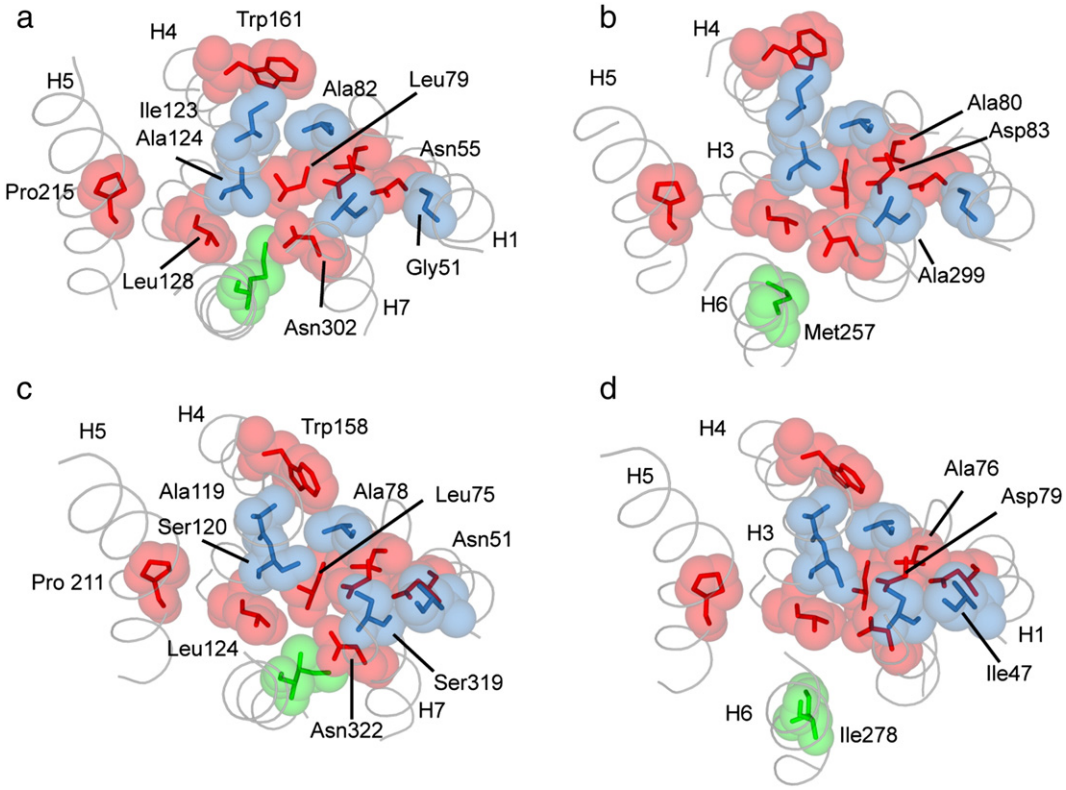


**Fig. 5.** Packing within the transmembrane core of rhodopsin and the β2AR. Cross sections are shown from the crystal structures of rhodopsin (PDB ID: 1U19) (a), active opsin (PDB ID: 3PQR) (b), inactive $\beta_2$AR (PDB ID: 2RH1) (c) and active $\beta_2$AR (PDB ID: 3SN6). The signature residues are highlighted in red and the group conserved residues in blue. Met257 (green) has high conservation within the subfamily of visual receptors and Ile278 (green) has high conservation within the subfamily of amine receptors.

change in the TM core is a closing of the space between Leu124 on H3 and Asn322 on H7 as Ile278 on H6 pivots away from the core. This change is not as marked as in rhodopsin, but still reflects an important ratcheting of H3 relative to H6 upon receptor activation.

The comparison between rhodopsin and the $\beta_2$AR highlights the important role that Met257 plays in rhodopsin. In fact, one of the strongest arguments that rhodopsin can serve as a model class A GPCR is that mutation of Met257 allows activation of opsin by the addition of all-*trans* retinal as a diffusible ligand [84]. That is, a single mutation in the TM core can convert the receptor into a ligand-activated receptor. Most substitutions of Met257 exhibit low, but measurable, activity without bound retinal. These receptors are locked off by covalent attachment of the "inverse agonist" 11-*cis* retinal, but exhibit activities comparable to the light activated receptor upon binding the "agonist" all-*trans* retinal. For example, the M257I mutation (where isoleucine is the wild-type residue in $\beta_2$AR) exhibits 4.4% opsin activity, 1.0% activity with bound 11-*cis* retinal and 71% activity with the addition of all-*trans* retinal. These results suggest that methionine at position 257 stabilizes the inactive state of rhodopsin, whereas isoleucine allows H6 to easily rotate into an active orientation upon "ligand" binding. More polar substitutions at position 257 in the M257Y, M257N, and M257S mutants appear to stabilize a direct interaction with Arg135, hold H6 in an active orientation and result in high levels of constitutive activity.

Fig. 6 presents the packing interactions involving Trp265 in rhodopsin. Trp265 is located between Gly121 on H3 and Ala295 on H6. Gly121 is highly conserved in the visual receptor subfamily, while Ala295 is a highly group conserved residue. Fig. 6b presents NMR spectra illustrating changes in Trp265 packing interactions between rhodopsin and Meta II.

## 4. Hydrogen bonding interactions between TM helices

The packing interactions of the seven TM helices influence the energy cost of moving helices relative to one another. Close helix–helix contacts allow stabilizing hydrogen-bonding interactions to form. In contrast, water can line the interfaces between more loosely packed helices, which allow helix motion. Table 2 lists inter-helical hydrogen-bonding interactions between the TM helices based on the crystal structures of rhodopsin and active opsin. Two of these contacts are highlighted in Fig. 7. The first hydrogen-bonding network involves the amide side chain of Asn55 (Fig. 7a). Asn55 is the most highly conserved residue in the class A GPCRs. The orientation of the side chain appears to be tightly controlled by the hydrogen bonding of the amide $NH_2$ protons to the backbone carbonyl oxygens of Gly51 and Ala299, two group conserved residues.

**Table 2**
Interhelical hydrogen bonding interactions in rhodopsin and active opsin[a].

| Interaction | Distance (angstroms) | |
|---|---|---|
| | 1GZM | 3CAP |
| *H1–H2* | | |
| Asn55(δ-O) – Asp83(δ-O) | 2.5 | 2.8 |
| *H1–H7* | | |
| Tyr43(OH) – Phe293(C=O) | 2.6 | – |
| Asn55(δ-N) – Ala299(C=O) | 2.9 | 2.9 |
| *H2–H3* | | |
| Asn78(δ-N) – Ser127(OH) | 3.5 | 2.9 |
| *H2–H4* | | |
| Tyr74(OH) – Glu150(ε-O) | 2.9 | – |
| Asn78(δ-O) – Trp161(ε-N) | 2.7 | 3.2 |
| Asn78(δ-N) – Thr160(OH) | 3.0 | 2.8 |
| *H2–H7* | | |
| Asn73(δ-N) – Tyr306(OH) | 3.2 | – |
| *H3–H5* | | |
| Glu122(ε-O) – His211(δ-N) | – | 3.2 |
| Glu122(ε-O) – His211(C=O) | 2.8 | |
| Trp126(ε-N) – His211(δ-N) | 3.3 | 3.3 |
| Arg135(η-N) – Tyr223(OH) | – | 2.7 |
| Tyr136(OH) – Gln225(ε-N) | 3.0 | – |
| *H3–H6* | | |
| Arg135(η-N) – Glu247(ε-O) | 2.9 | – |
| Arg135(η-N) – Glu247(C=O) | 3.4 | – |
| *H3–H7* | | |
| Glu113(ε-O) – Lys296(ζ-N) | 3.2 | – |
| *H4–H5* | | |
| Ala166(C=O) – Tyr206(OH) | 2.6 | 2.9 |
| *H5–H6* | | |
| Lys231(ζ-N) – Thr251(OH) | – | 2.8 |
| Lys231(ζ-N) – Glu247(ε-O) | – | 3.0 |
| Ala234(C=O) – Gln244(ε-N) | – | 3.4 |

[a] A cutoff of 3.5 Å between heteroatoms was used for inferring interhelical hydrogen bonding interactions. In crystal structures, the protons within hydrogen bonds are not directly observed.

A second example of inter-helical hydrogen bonding contacts involves the interaction of the Glu122 carboxyl group on H3 with the backbone carbonyl of His211 (Fig. 7c and d). The His211 carbonyl is free to hydrogen bond due to the presence of proline at position 215. Activation of the rhodopsin leads to a shift of the hydrogen bonding contacts from the backbone C=O to the side chain imidazole in Meta II.

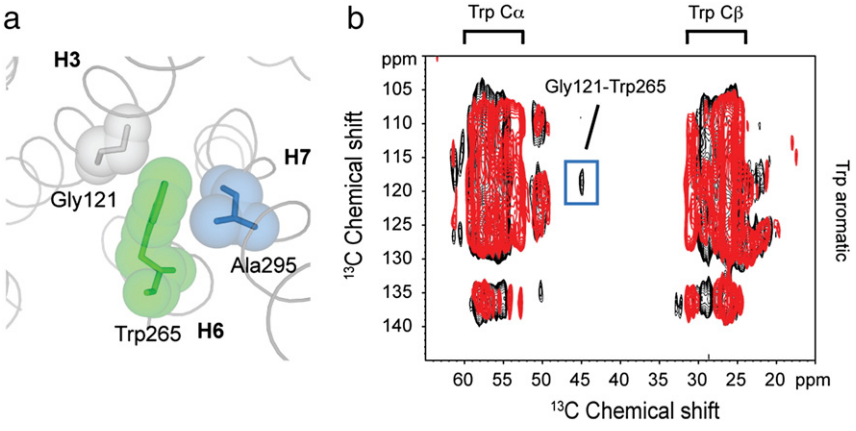


**Fig. 6.** Packing interactions involving Trp265 in rhodopsin. (a) Trp265 is located between Gly121 on H3 and Ala295 on H6 in rhodopsin (PDB ID: 1GZM). (b) NMR spectra illustrating changes in Trp265 packing interactions between rhodopsin and Meta II. Activation results in loss of a cross peak between Gly121 on H3 and the indole ring of Trp265 on H6.

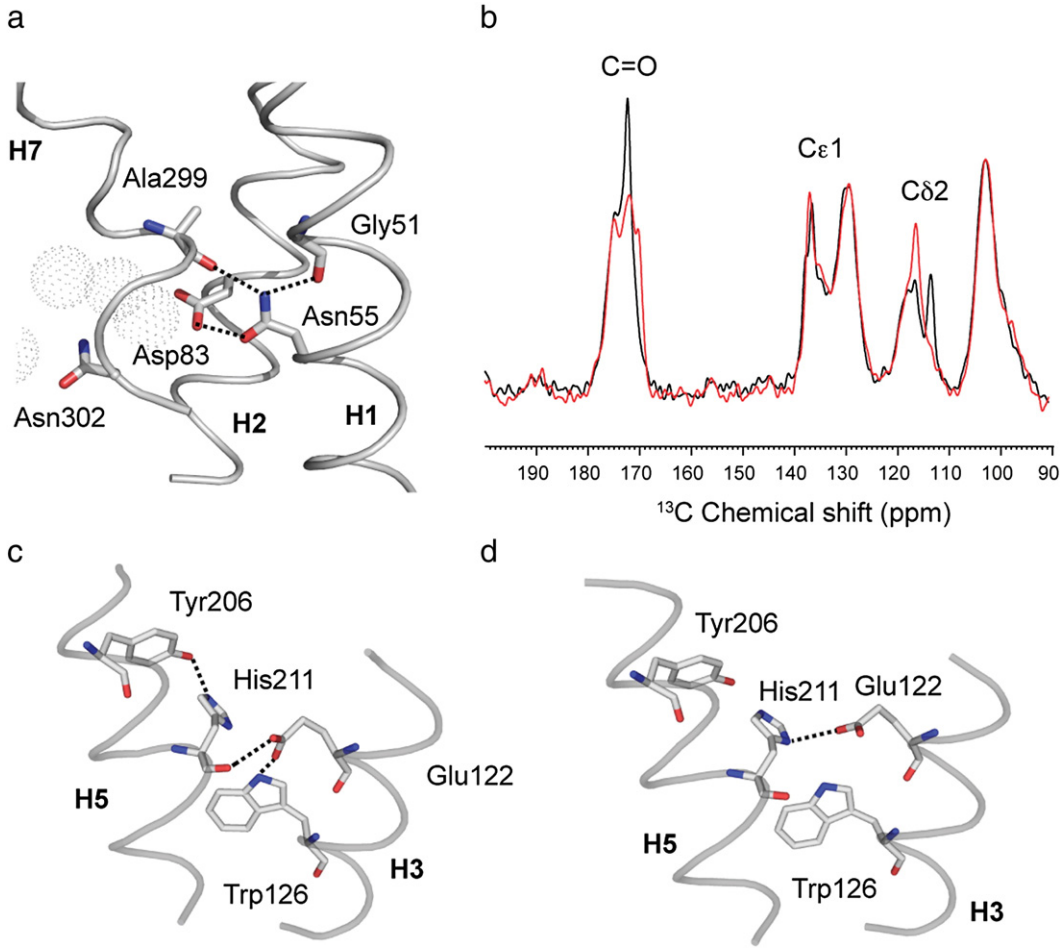


**Fig. 7.** Hydrogen bonding interactions between TM helices in rhodopsin. (a) Hydrogen bonding between the backbone carbonyl oxygens of Gly51 and Ala299 and the amide group of Asn55 serves to orient the Asn55 side chain in rhodopsin (PDB ID: 1U19). (b) One-dimensional $^{13}C$ spectra of rhodopsin (black) and Meta II (red) labeled with U-$^{13}C$-labeled histidine. Hydrogen bonding interactions between Glu122 and His211 are reflected by the changes in the C=O and Cδ2 chemical shifts. (c) Hydrogen bonding interactions between Glu122, Trp126 and His211 in rhodopsin (PDB ID: 1U19). (d) Changes in hydrogen bonding between Glu122, Trp126 and His211 following activation in Meta II (PDB ID: 3PQR).

Fig. 7b shows that the changes in hydrogen bonding of His211 lead to distinctive changes in $^{13}C$ chemical shifts. Hydrogen bonding changes lead changes in the electron density about associated $^{13}C$ atoms, and these in turn are reflected in changes in chemical shifts [85,86]. When viewed from the extracellular surface of rhodopsin, the retinal β-ionone ring is packed against Glu122. Retinal movement disrupts the hydrogen bond between the main chain carbonyl of His211 and the side-chain of Glu122, and a new hydrogen bond forms between Glu122 and the imidazole δ-nitrogen of His211. A direct side-chain interaction explains mutational data on His211 that point to a role of the His211 side-chain in Meta II stability and activation [87]. Both NMR measurements and X-ray crystal structures of active opsin and Meta II indicate that the position of the ring has shifted toward helix H5 in Meta II. The shift in the position of the retinal is likely a consequence of isomerization to the longer all-*trans* configuration as well as the coupled motion of EL2 and H5. These observations are consistent with studies using retinal analogs that show that the β-ionone ring is required for rhodopsin activation [88,89].

## 5. Electrostatic interactions within the TM region of rhodopsin

Charged residues within the interior of membrane proteins are often functionally important. There are two key electrostatic interactions within the TM region of rhodopsin. These interactions correspond to the retinal PSB and its negatively charged counterion, and the electrostatic interaction connecting Arg135 to Glu134 and Glu247.

Fig. 8 presents the structure of rhodopsin showing the location of Trp265 relative to the retinal chromophore, TM core and two protonation switches responsible for rhodopsin activation. The conserved TM core lies between the Glu113–PSB salt bridge on the extracellular side of the receptor and the Arg135 – Glu247 "ionic lock" on the cytoplasmic side of the receptor. There is a growing body of evidence that these two ionic pairs function as protonation switches that control rhodopsin activation [50]. Internal proton transfer occurs from the retinal PSB to Glu113 upon activation, which allows H6 to pivot and rotate outward on the intracellular side of rhodopsin. This motion of H6 breaks the ionic lock on the intracellular side of the protein and allows the uptake of a proton from the solvent by Glu134, thereby stabilizing the active state. The sequence of events in the activation mechanism (i.e., protonation of Glu113 by an internal proton transfer, an outward rotation of H6 and protonation of Glu134) is associated with a series of Meta II substates [75].

In many receptor subfamilies, the classic ionic lock between Arg135 and Glu247 is absent. For example, in the chemokine receptors the intracellular end of H6 is highly positively charged and lacks a negatively charged residue at or near position of this glutamate. Instead, there are two highly subfamily conserved residues (Thr 97%; Asp 85%) at the intracellular end of H2 that are positioned close to the arginine of the E/DRY motif in homology models of the chemokine receptors. These

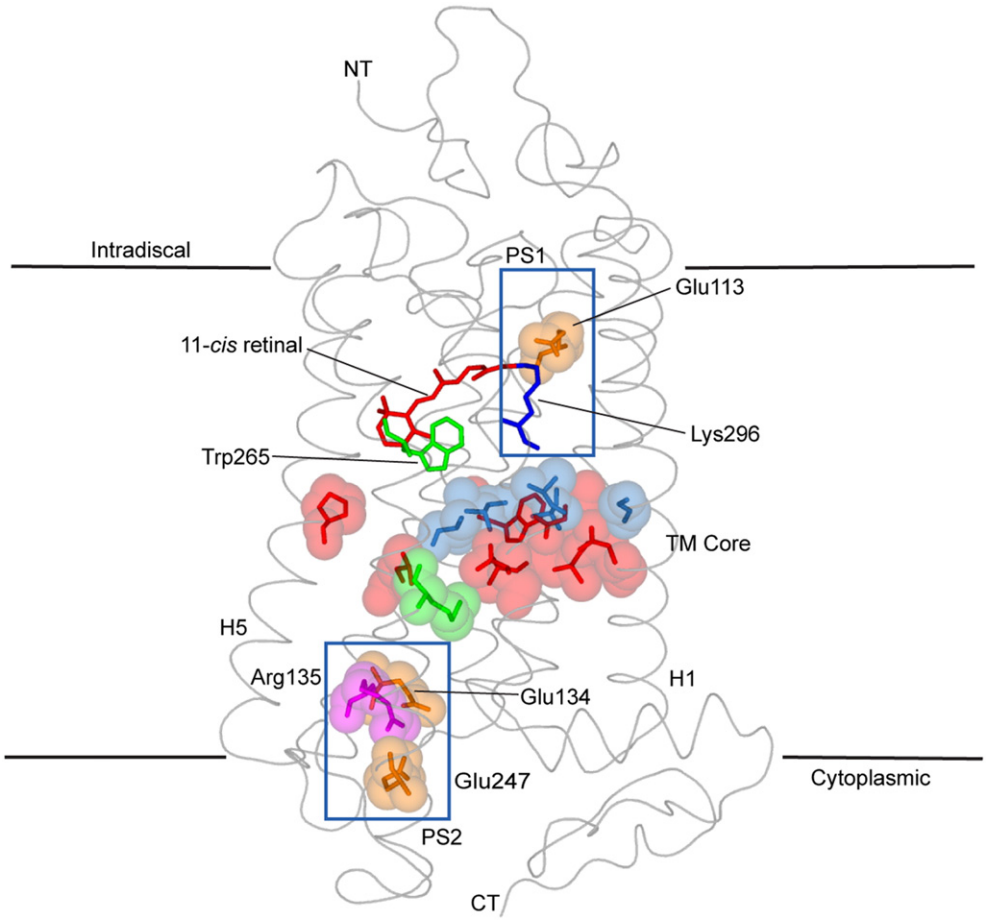


**Fig. 8.** Structure of rhodopsin. The conserved TM core lies between the two protonation switches (PS1 and PS2, blue boxes) required for receptor activation [50]. The first protonation switch involves a proton transfer from the retinal PSB to Glu113. The second protonation switch involves the protonation of Glu134 from the cytoplasm. It is thought that both protonation switches are shielded from bulk water [91], which would increase the interaction energy between complementary charges. Rhodopsin structure is shown using PDB ID: IU19.

residues may replace glutamic acid on H6 to stabilize the inactive receptor conformation. Chemokine receptors also have low conservation (52%) of the tyrosine in the NPxxY motif on H7 consistent with a different type of intracellular ionic lock. Nevertheless, conservation of the transmembrane core and the conserved Tyr223 on H5 suggests that the signaling pathway is not dramatically different from that described for rhodopsin. These and other examples emphasize the interplay of the signature, group-conserved and subfamily conserved amino acids in understanding the similarities and differences in how the class A GPCRs are activated.

## Acknowledgements

This work was supported by a grant from the National Institutes of Health (RO1-GM41412).

## References

[1] G.B. Cohen, T. Yang, P.R. Robinson, D.D. Oprian, Constitutive activation of opsin: influence of charge at position 134 and size at position 296, Biochemistry 32 (1993) 6111–6115.
[2] R. Vogel, F. Siebert, Conformations of the active and inactive states of opsin, J. Biol. Chem. 276 (2001) 38487–38493.
[3] R.W. Schoenlein, L.A. Peteanu, R.A. Mathies, C.V. Shank, The first step in vision: femtosecond isomerization of rhodopsin, Science 254 (1991) 412–415.
[4] H. Imai, D. Kojima, T. Oura, S. Tachibanaki, A. Terakita, Y. Shichida, Single amino acid residue as a functional determinant of rod and cone visual pigments, Proc. Natl. Acad. Sci. U. S. A. 94 (1997) 2322–2326.
[5] D.L. Farrens, C. Altenbach, K. Yang, W.L. Hubbell, H.G. Khorana, Requirement of rigid-body motion of transmembrane helices for light activation of rhodopsin, Science 274 (1996) 768–770.
[6] J.H. Park, P. Scheerer, K.P. Hofmann, H.W. Choe, O.P. Ernst, Crystal structure of the ligand-free G-protein-coupled receptor opsin, Nature 454 (2008) 183–187.
[7] P. Scheerer, J.H. Park, P.W. Hildebrand, Y.J. Kim, N. Krauss, H.W. Choe, K.P. Hofmann, O.P. Ernst, Crystal structure of opsin in its G-protein-interacting conformation, Nature 455 (2008) 497–502.
[8] K. Palczewski, T. Kumasaka, T. Hori, C.A. Behnke, H. Motoshima, B.A. Fox, I. Le Trong, D.C. Teller, T. Okada, R.E. Stenkamp, M. Yamamoto, M. Miyano, Crystal structure of rhodopsin: a G protein-coupled receptor, Science 289 (2000) 739–745.
[9] H.W. Choe, Y.J. Kim, J.H. Park, T. Morizumi, E.F. Pai, N. Krauss, K.P. Hofmann, P. Scheerer, O.P. Ernst, Crystal structure of Metarhodopsin II, Nature 471 (2011) 651–655.
[10] M. Murakami, T. Kouyama, Crystal structure of squid rhodopsin, Nature 453 (2008) 363–367.
[11] J.F. White, N. Noinaj, Y. Shibata, J. Love, B. Kloss, F. Xu, J. Gvozdenovic-Jeremic, P. Shah, J. Shiloach, C.G. Tate, R. Grisshammer, Structure of the agonist-bound neurotensin receptor, Nature 490 (2012) 508–513.
[12] D. Wacker, C. Wang, V. Katritch, G.W. Han, X.-P. Huang, E. Vardy, J.D. McCorvy, Y. Jiang, M. Chu, F.Y. Siu, W. Liu, H.E. Xu, V. Cherezov, B.L. Roth, R.C. Stevens, Structural features for functional selectivity at serotonin receptors, Science 340 (2013) 615–619.
[13] C. Wang, Y. Jiang, J. Ma, H. Wu, D. Wacker, V. Katritch, G.W. Han, W. Liu, X.-P. Huang, E. Vardy, J.D. McCorvy, X. Gao, X.E. Zhou, K. Melcher, C. Zhang, F. Bai, H. Yang, L. Yang, H. Jiang, B.L. Roth, V. Cherezov, R.C. Stevens, H.E. Xu, Structural basis for molecular recognition at serotonin receptors, Science 340 (2013) 610–614.
[14] T. Shimamura, M. Shiroishi, S. Weyand, H. Tsujimoto, G. Winter, V. Katritch, R. Abagyan, V. Cherezov, W. Liu, G.W. Han, T. Kobayashi, R.C. Stevens, S. Iwata, Structure of the human histamine $H_1$ receptor complex with doxepin, Nature 475 (2011) 65–70.
[15] F. Xu, H.X. Wu, V. Katritch, G.W. Han, K.A. Jacobson, Z.G. Gao, V. Cherezov, R.C. Stevens, Structure of an agonist-bound human $A_{2A}$ adenosine receptor, Science 332 (2011) 322–327.
[16] E.Y.T. Chien, W. Liu, Q.A. Zhao, V. Katritch, G.W. Han, M.A. Hanson, L. Shi, A.H. Newman, J.A. Javitch, V. Cherezov, R.C. Stevens, Structure of the human dopamine D3 receptor in complex with a D2/D3 selective antagonist, Science 330 (2010) 1091–1095.

[17] D. Wacker, G. Fenalti, M.A. Brown, V. Katritch, R. Abagyan, V. Cherezov, R.C. Stevens, Conserved binding mode of human $\beta_2$ adrenergic receptor inverse agonists and antagonist revealed by X-ray crystallography, J. Am. Chem. Soc. 132 (2010) 11443–11445.

[18] V.P. Jaakola, M.T. Griffith, M.A. Hanson, V. Cherezov, E.Y.T. Chien, J.R. Lane, A.P. Ijzerman, R.C. Stevens, The 2.6 Angstrom crystal structure of a human $A_{2A}$ adenosine receptor bound to an antagonist, Science 322 (2008) 1211–1217.

[19] S.G.F. Rasmussen, H.J. Choi, D.M. Rosenbaum, T.S. Kobilka, F.S. Thian, P.C. Edwards, M. Burghammer, V.R.P. Ratnala, R. Sanishvili, R.F. Fischetti, G.F.X. Schertler, W.I. Weis, B.K. Kobilka, Crystal structure of the human $\beta_2$ adrenergic G-protein-coupled receptor, Nature 450 (2007) 383–387.

[20] V. Cherezov, D.M. Rosenbaum, M.A. Hanson, S.G.F. Rasmussen, F.S. Thian, T.S. Kobilka, H.J. Choi, P. Kuhn, W.I. Weis, B.K. Kobilka, R.C. Stevens, High-resolution crystal structure of an engineered human $\beta_2$-adrenergic G protein-coupled receptor, Science 318 (2007) 1258–1265.

[21] T. Warne, M.J. Serrano-Vega, J.G. Baker, R. Moukhametzianov, P.C. Edwards, R. Henderson, A.G. Leslie, C.G. Tate, G.F.X. Schertler, Structure of a $\beta_1$-adrenergic G-protein-coupled receptor, Nature 454 (2008) 486–491.

[22] B. Wu, E.Y. Chien, C.D. Mol, G. Fenalti, W. Liu, V. Katritch, R. Abagyan, A. Brooun, P. Wells, F.C. Bi, D.J. Hamel, P. Kuhn, T.M. Handel, V. Cherezov, R.C. Stevens, Structures of the CXCR4 chemokine GPCR with small-molecule and cyclic peptide antagonists, Science 330 (2010) 1066–1071.

[23] A.C. Kruse, J. Hu, A.C. Pan, D.H. Arlow, D.M. Rosenbaum, E. Rosemond, H.F. Green, T. Liu, P.S. Chae, R.O. Dror, D.E. Shaw, W.I. Weis, J. Wess, B.K. Kobilka, Structure and dynamics of the M3 muscarinic acetylcholine receptor, Nature 482 (2012) 552–556.

[24] K. Haga, A.C. Kruse, H. Asada, T. Yurugi-Kobayashi, M. Shiroishi, C. Zhang, W.I. Weis, T. Okada, B.K. Kobilka, T. Haga, T. Kobayashi, Structure of the human M2 muscarinic acetylcholine receptor bound to an antagonist, Nature 482 (2012) 547–551.

[25] H. Wu, D. Wacker, M. Mileni, V. Katritch, G.W. Han, E. Vardy, W. Liu, A.A. Thompson, X.-P. Huang, F.I. Carroll, S.W. Mascarella, R.B. Westkaemper, P.D. Mosier, B.L. Roth, V. Cherezov, R.C. Stevens, Structure of the human κ-opioid receptor in complex with JDTic, Nature 485 (2012) 327–332.

[26] A.A. Thompson, W. Liu, E. Chun, V. Katritch, H. Wu, E. Vardy, X.-P. Huang, C. Trapella, R. Guerrini, G. Calo, B.L. Roth, V. Cherezov, R.C. Stevens, Structure of the nociceptin/orphanin FQ receptor in complex with a peptide mimetic, Nature 485 (2012) 395–399.

[27] A. Manglik, A.C. Kruse, T.S. Kobilka, F.S. Thian, J.M. Mathiesen, R.K. Sunahara, L. Pardo, W.I. Weis, B.K. Kobilka, S. Granier, Crystal structure of the μ-opioid receptor bound to a morphinan antagonist, Nature 485 (2012) 321–326.

[28] S. Granier, A. Manglik, A.C. Kruse, T.S. Kobilka, F.S. Thian, W.I. Weis, B.K. Kobilka, Structure of the δ-opioid receptor bound to naltrindole, Nature 485 (2012) 400–404.

[29] M.A. Hanson, C.B. Roth, E. Jo, M.T. Griffith, F.L. Scott, G. Reinhart, H. Desale, B. Clemons, S.M. Cahalan, S.C. Schuerer, M.G. Sanna, G.W. Han, P. Kuhn, H. Rosen, R.C. Stevens, Crystal structure of a lipid G protein-coupled receptor, Science 335 (2012) 851–855.

[30] C. Zhang, Y. Srinivasan, D.H. Arlow, J.J. Fung, D. Palmer, Y. Zheng, H.F. Green, A. Pandey, R.O. Dror, D.E. Shaw, W.I. Weis, S.R. Coughlin, B.K. Kobilka, High-resolution crystal structure of human protease-activated receptor 1, Nature 492 (2012) 387–392.

[31] S.G.F. Rasmussen, H.J. Choi, J.J. Fung, E. Pardon, P. Casarosa, P.S. Chae, B.T. DeVree, D.M. Rosenbaum, F.S. Thian, T.S. Kobilka, A. Schnapp, I. Konetzki, R.K. Sunahara, S.H. Gellman, A. Pautsch, J. Steyaert, W.I. Weis, B.K. Kobilka, Structure of a nanobody-stabilized active state of the $\beta_2$ adrenoceptor, Nature 469 (2011) 175–180.

[32] S.G.F. Rasmussen, B.T. DeVree, Y. Zou, A.C. Kruse, K.Y. Chung, T.S. Kobilka, F.S. Thian, P.S. Chae, E. Pardon, D. Calinski, J.M. Mathiesen, S.T.A. Shah, J.A. Lyons, M. Caffrey, S.H. Gellman, J. Steyaert, G. Skiniotis, W.I. Weis, R.K. Sunahara, B.K. Kobilka, Crystal structure of the $\beta_2$ adrenergic receptor-Gs protein complex, Nature 477 (2011) 549–555.

[33] T. Warne, P.C. Edwards, A.G.W. Leslie, C.G. Tate, Crystal structures of a stabilized beta(1)-adrenoceptor bound to the biased agonists bucindolol and carvedilol, Structure 20 (2012) 841–849.

[34] B.K. Kobilka, X. Deupi, Conformational complexity of G-protein-coupled receptors, Trends Pharmacol. Sci. 28 (2007) 397–406.

[35] G. Lebon, T. Warne, P.C. Edwards, K. Bennett, C.J. Langmead, A.G.W. Leslie, C.G. Tate, Agonist-bound adenosine $A_{2A}$ receptor structures reveal common features of GPCR activation, Nature 474 (2011) 521–525.

[36] T. Warne, R. Moukhametzianov, J.G. Baker, R. Nehmé, P.C. Edwards, A.G.W. Leslie, G.F.X. Schertler, C.G. Tate, The structural basis for agonist and partial agonist action on a $\beta_1$-adrenergic receptor, Nature 469 (2011) 241–244.

[37] D.M. Rosenbaum, C. Zhang, J.A. Lyons, R. Holl, D. Aragao, D.H. Arlow, S.G.F. Rasmussen, H.J. Choi, B.T. DeVree, R.K. Sunahara, P.S. Chae, S.H. Gellman, R.O. Dror, D.E. Shaw, W.I. Weis, M. Caffrey, P. Gmeiner, B.K. Kobilka, Structure and function of an irreversible agonist-$\beta_2$ adrenoceptor complex, Nature 469 (2011) 236–240.

[38] K.Y. Chung, S.G.F. Rasmussen, T. Liu, S. Li, B.T. DeVree, P.S. Chae, D. Calinski, B.K. Kobilka, V.L. Woods Jr., R.K. Sunahara, Conformational changes in the G protein Gs induced by the $\beta_2$ adrenergic receptor, Nature 477 (2011) 611–615.

[39] K. Sansuk, X. Deupi, I.R. Torrecillas, A. Jongejan, S. Nijmeijer, R.A. Bakker, L. Pardo, R. Leurs, A structural insight into the reorientation of transmembrane domains 3 and 5 during family A G protein-coupled receptor activation, Mol. Pharmacol. 79 (2011) 262–269.

[40] X. Deupi, J. Standfuss, Structural insights into agonist-induced activation of G-protein-coupled receptors, Curr. Opin. Struct. Biol. 21 (2011) 541–551.

[41] B. Mertz, A.V. Struts, S.E. Feller, M.F. Brown, Molecular simulations and solid-state NMR investigate dynamical structure in rhodopsin activation, Biochim. Biophys. Acta Biomembr. 1818 (2012) 241–251.

[42] S.R. Kiihne, A.F.L. Creemers, W.J. de Grip, P.H.M. Bovee-Geurts, J. Lugtenburg, H.J.M. de Groot, Selective interface detection: mapping binding site contacts in membrane proteins by NMR spectroscopy, J. Am. Chem. Soc. 127 (2005) 5734–5735.

[43] A.F.L. Creemers, S. Kiihne, P.H.M. Bovee-Geurts, W.J. DeGrip, J. Lugtenburg, H.J.M. de Groot, $^{1}H$ and $^{13}C$ MAS NMR evidence for pronounced ligand–protein interactions involving the ionone ring of the retinylidene chromophore in rhodopsin, Proc. Natl. Acad. Sci. U. S. A. 99 (2002) 9101–9106.

[44] M. Concistrè, O.G. Johannessen, N. McLean, P.H.M. Bovee-Geurts, R.C.D. Brown, W.J. DeGrip, M.H. Levitt, A large geometric distortion in the first photointermediate of rhodopsin, determined by double-quantum solid-state NMR, J. Biomol. NMR 53 (2012) 247–256.

[45] J.A. Goncalves, S. Ahuja, S. Erfani, M. Eilers, S.O. Smith, Structure and function of G protein-coupled receptors using NMR spectroscopy, Prog. Nucl. Magn. Reson. Spectrosc. 57 (2010) 159–180.

[46] M. Concistre, O.G. Johannessen, E. Carignani, M. Geppi, M.H. Levitt, Magic-angle spinning NMR of cold samples, Acc. Chem. Res. 46 (2013) 1914–1922.

[47] W. Liu, M. Eilers, A.B. Patel, S.O. Smith, Helix packing moments reveal diversity and conservation in membrane protein structure, J. Mol. Biol. 337 (2004) 713–729.

[48] M. Eilers, A.B. Patel, W. Liu, S.O. Smith, Comparison of helix interactions in membrane and soluble α-bundle proteins, Biophys. J. 82 (2002) 2720–2736.

[49] E. Crocker, M. Eilers, S. Ahuja, V. Hornak, A. Hirshfeld, M. Sheves, S.O. Smith, Location of Trp265 in Metarhodopsin II: implications for the activation mechanism of the visual receptor rhodopsin, J. Mol. Biol. 357 (2006) 163–172.

[50] M. Mahalingam, K. Martinez-Mayorga, M.F. Brown, R. Vogel, Two protonation switches control rhodopsin activation in membranes, Proc. Natl. Acad. Sci. U. S. A. 105 (2008) 17795–17800.

[51] G.F.J. Salgado, A.V. Struts, K. Tanaka, S. Krane, K. Nakanishi, M.F. Brown, Solid-state $^{2}H$ NMR structure of retinal in Metarhodopsin I, J. Am. Chem. Soc. 128 (2006) 11067–11071.

[52] G.F.J. Salgado, A.V. Struts, K. Tanaka, N. Fujioka, K. Nakanishi, M.F. Brown, Deuterium NMR structure of retinal in the ground state of rhodopsin, Biochemistry 43 (2004) 12819–12828.

[53] A.V. Struts, G.F.J. Salgad, K. Tanaka, S. Krane, K. Nakanishi, M.F. Brown, Structural analysis and dynamics of retinal chromophore in dark and Meta I states of rhodopsin from $^{2}H$ NMR of aligned membranes, J. Mol. Biol. 372 (2007) 50–66.

[54] T. Okada, M. Sugihara, A.N. Bondar, M. Elstner, P. Entel, V. Buss, The retinal conformation and its environment in rhodopsin in light of a new 2.2 Å crystal structure, J. Mol. Biol. 342 (2004) 571–583.

[55] M. Sugihara, J. Hufen, V. Buss, Origin and consequences of steric strain in the rhodopsin binding pocket, Biochemistry 45 (2006) 801–810.

[56] X. Feng, P.J.E. Verdegem, Y.K. Lee, D. Sandström, M. Eden, P. Bovee-Geurts, W.J. Degrip, J. Lugtenburg, H.J.M. Degroot, M.H. Levitt, Direct determination of a molecular torsional angle in the membrane protein rhodopsin by solid-state NMR, J. Am. Chem. Soc. 119 (1997) 6853–6857.

[57] X. Feng, P.J.E. Verdegem, M. Eden, D. Sandström, Y.K. Lee, P.H.M. Bovee-Geurts, W.J. De Grip, J. Lugtenburg, H.J.M. de Groot, M.H. Levitt, Determination of a molecular torsional angle in the Metarhodopsin-I photointermediate of rhodopsin by double-quantum solid-state NMR, J. Biomol. NMR 16 (2000) 1–8.

[58] P.J.E. Verdegem, P.H.M. Bovee-Geurts, W.J. De Grip, J. Lugtenburg, H.J.M. de Groot, Retinylidene ligand structure in bovine rhodopsin, Metarhodopsin-I, and 10-methylrhodopsin from internuclear distance measurements using C-13-labeling and 1-D rotational resonance MAS NMR, Biochemistry 38 (1999) 11316–11324.

[59] Q. Wang, G.G. Kochendoerfer, R.W. Schoenlein, P.J.E. Verdegem, J. Lugtenburg, R.A. Mathies, C.V. Shank, Femtosecond spectroscopy of a 13-demethylrhodopsin visual pigment analogue: the role of nonbonded interactions in the isomerization process, J. Phys. Chem. 100 (1996) 17388–17394.

[60] G.G. Kochendoerfer, P.J.E. Verdegem, I. van der Hoef, J. Lugtenburg, R.A. Mathies, Retinal analog study of the role of steric interactions in the excited state isomerization dynamics of rhodopsin, Biochemistry 35 (1996) 16230–16240.

[61] D.W. Corson, M.C. Cornwall, E.F. MacNichol, S. Tsang, F. Derguini, R.K. Crouch, K. Nakanishi, Relief of opsin desensitization and prolonged excitation of rod photoreceptors by 9-desmethylretinal, Proc. Natl. Acad. Sci. U. S. A. 91 (1994) 6958–6962.

[62] M. Han, M. Groesbeek, T.P. Sakmar, S.O. Smith, The C9 methyl group of retinal interacts with glycine-121 in rhodopsin, Proc. Natl. Acad. Sci. U. S. A. 94 (1997) 13442–13447.

[63] J. Goncalves, M. Eilers, K. South, C.A. Opefi, P. Laissue, P.J. Reeves, S.O. Smith, Magic angle spinning nuclear magnetic resonance spectroscopy of G protein-coupled receptors, Methods Enzymol. 522 (2013) 365–389.

[64] D.P. Raleigh, M.H. Levitt, R.G. Griffin, Rotational resonance in solid state NMR, Chem. Phys. Lett. 146 (1988) 71–76.

[65] T. Gullion, J. Schaefer, Detection of weak heteronuclear dipolar coupling by rotational-echo double-resonance NMR, in: W.S. Warren (Ed.), Advances in Magnetic Resonance, Conference on "High Resolution NMR in Solids", January 19–21, 1989, vol. 13, Academic Press, Inc., San Diego, California, USA; London, England, UK, 1989, pp. 57–84.

[66] A.E. Bennett, J.H. Ok, R.G. Griffin, S. Vega, Chemical-shift correlation spectroscopy in rotating solids — radio frequency-driven dipolar recoupling and longitudinal exchange, J. Chem. Phys. 96 (1992) 8624–8627.

[67] D.K. Sodickson, M.H. Levitt, S. Vega, R.G. Griffin, Broad-band dipolar recoupling in the nuclear-magnetic-resonance of rotating solids, J. Chem. Phys. 98 (1993) 6742–6748.

[68] Y.K. Lee, N.D. Kurur, M. Helmle, O.G. Johannessen, N.C. Nielsen, M.H. Levitt, Efficient dipolar recoupling in the NMR of rotating solids. A sevenfold symmetric radiofrequency pulse sequence, Chem. Phys. Lett. 242 (1995) 304–309.

[69] C.M. Rienstra, M.E. Hatcher, L.J. Mueller, B.Q. Sun, S.W. Fesik, R.G. Griffin, Efficient multispin homonuclear double-quantum recoupling for magic-angle spinning

NMR: C-13-C-13 correlation spectroscopy of U-C-13-erythromycin A, J. Am. Chem. Soc. 120 (1998) 10602–10612.
[70] K. Takegoshi, S. Nakamura, T. Terao, $^{13}C$–$^{1}H$ dipolar-assisted rotational resonance in magic-angle spinning NMR, Chem. Phys. Lett. 344 (2001) 631–637.
[71] E. Crocker, A.B. Patel, M. Eilers, S. Jayaraman, E. Getmanova, P.J. Reeves, M. Ziliox, H.G. Khorana, M. Sheves, S.O. Smith, Dipolar assisted rotational resonance NMR of tryptophan and tyrosine in rhodopsin, J. Biomol. NMR 29 (2004) 11–20.
[72] J. Standfuss, P.C. Edwards, A. D'Antona, M. Fransen, G. Xie, D.D. Oprian, G.F. Schertler, The structural basis of agonist-induced activation in constitutively active rhodopsin, Nature 471 (2011) 656–660.
[73] X. Deupi, P. Edwards, A. Singhal, B. Nickle, D. Oprian, G. Schertler, J. Standfuss, Stabilized G protein binding site in the structure of constitutively active Metarhodopsin — II, Proc. Natl. Acad. Sci. U. S. A. 109 (2012) 119–124.
[74] F. Castellani, B. van Rossum, A. Diehl, M. Schubert, K. Rehbein, H. Oschkinat, Structure of a protein determined by solid-state magic-angle-spinning NMR spectroscopy, Nature 420 (2002) 98–102.
[75] B. Knierim, K.P. Hofmann, O.P. Ernst, W.L. Hubbell, Sequence of late molecular events in the activation of rhodopsin, Proc. Natl. Acad. Sci. U. S. A. 104 (2007) 20290–20295.
[76] S. Ahuja, M. Eilers, A. Hirshfeld, E.C.Y. Yan, M. Ziliox, T.P. Sakmar, M. Sheves, S.O. Smith, 6-s-*cis* conformation and polar binding pocket of the retinal chromophore in the photoactivated state of rhodopsin, J. Am. Chem. Soc. 131 (2009) 15160–15169.
[77] M. Chabre, J. Breton, Orientation of aromatic residues in rhodopsin. Rotation of one tryptophan upon the Meta I to Meta II transition after illumination, Photochem. Photobiol. 30 (1979) 295–299.
[78] C.N. Rafferty, C.G. Muellenberg, H. Shichi, Tryptophan in bovine rhodopsin: its content, spectral properties, and environment, Biochemistry 19 (1980) 2145–2151.
[79] S.W. Lin, T.P. Sakmar, Specific tryptophan UV-absorbance changes are probes of the transition of rhodopsin to its active state, Biochemistry 35 (1996) 11149–11159.
[80] G.G. Kochendoerfer, S. Kaminaka, R.A. Mathies, Ultraviolet resonance Raman examination of the light-induced protein structural changes in rhodopsin activation, Biochemistry 36 (1997) 13153–13159.
[81] A.B. Patel, E. Crocker, P.J. Reeves, E.V. Getmanova, M. Eilers, H.G. Khorana, S.O. Smith, Changes in interhelical hydrogen bonding upon rhodopsin activation, J. Mol. Biol. 347 (2005) 803–812.
[82] K. Werner, I. Lehner, H.K. Dhiman, C. Richter, C. Glaubitz, H. Schwalbe, J. Klein-Seetharaman, H.G. Khorana, Combined solid state and solution NMR studies of α, ε-$^{15}N$ labeled bovine rhodopsin, J. Biomol. NMR 37 (2007) 303–312.
[83] A.T. Petkova, M. Hatanaka, C.P. Jaroniec, J.G.G. Hu, M. Belenky, M. Verhoeven, J. Lugtenburg, R.G. Griffin, J. Herzfeld, Tryptophan interactions in bacteriorhodopsin: a heteronuclear solid-state NMR study, Biochemistry 41 (2002) 2429–2437.
[84] M. Han, S.O. Smith, T.P. Sakmar, Constitutive activation of opsin by mutation of methionine 257 on transmembrane helix 6, Biochemistry 37 (1998) 8253–8261.
[85] Z.T. Gu, R. Zambrano, A. McDermott, Hydrogen-bonding of carboxyl groups in solid state amino acids and peptides: comparison of carbon chemical shielding, infrared frequencies, and structures, J. Am. Chem. Soc. 116 (1994) 6368–6372.
[86] Y.F. Wei, A.C. de Dios, A.E. McDermott, Solid-state $^{15}N$ NMR chemical shift anisotropy of histidines: experimental and theoretical studies of hydrogen bonding, J. Am. Chem. Soc. 121 (1999) 10389–10394.
[87] J.W. Lewis, I. Szundi, M.A. Kazmi, T.P. Sakmar, D.S. Kliger, Proton movement and photointermediate kinetics in rhodopsin mutants, Biochemistry 45 (2006) 5430–5439.
[88] F. Jäger, S. Jäger, O. Kräutle, N. Friedman, M. Sheves, K.P. Hofmann, F. Siebert, Interactions of the β-ionone ring with the protein in the visual pigment rhodopsin control the activation mechanism. An FTIR and fluorescence study on artificial vertebrate rhodopsins, Biochemistry 33 (1994) 7389–7397.
[89] R. Vogel, F. Siebert, S. Lüdeke, A. Hirshfeld, M. Sheves, Agonists and partial agonists of rhodopsin: retinals with ring modifications, Biochemistry 44 (2005) 11684–11699.
[90] N. Pattabiraman, K.B. Ward, P.J. Fleming, Occluded molecular surface: analysis of protein packing, J. Mol. Recognit. 8 (1995) 334–344.
[91] J. Ballesteros, S. Kitanovic, F. Guarnieri, P. Davies, B.J. Fromme, K. Konvicka, L. Chi, R.P. Millar, J.S. Davidson, H. Weinstein, S.C. Sealfon, Functional microdomains in G-protein-coupled receptors — the conserved arginine-cage motif in the gonadotropin-releasing hormone receptor, J. Biol. Chem. 273 (1998) 10445–10453.